# Visibility Estimation Using a Single Image

Qin Li and Bin Xie(✉)

School of Information Science and Engineering, Central South University, Changsha 410083, China
xiebin@csu.edu.cn

**Abstract.** In this paper, we propose a novel method for visibility estimation using only a single image as input. An assumption is proposed: the extinction coefficient of light is approximately a constant in clear atmosphere. Using this assumption with the theory of atmospheric radiation, the extinction coefficient in clear atmosphere can be estimated. Based on the dark channel prior, ratio of two extinction coefficients in current and clear atmosphere is calculated. By multiplying the clear extinction coefficient and the ratio, we can estimate the extinction coefficient of the input image and then obtain the visibility value. Compared with other methods that require the explicit extraction of the scene, our method needs no constraint and performs well in various types of scenes, which might open a new trend of visibility measurement in meteorological research. Moreover, the actual distance information can also be estimated as a by-product of this method.

**Keywords:** Clear atmosphere · Extinction coefficient
Dark channel prior · Visibility

## 1 Introduction

Visibility is an indicator of atmosphere transparency, which is closely related to our daily lives in many ways, like road safety applications, meteorological observation, airport safety and monitoring pollution in urban areas.

Little work has been done on visibility estimation based on outdoor cameras. There are two classes of methods. The first one is to estimate the distance to the most distant object on the road surface having a contrast above 5%. Pomerleau [19] measures the contrast attenuation of road markings at various distances in front of a moving vehicle for visibility estimation, which requires detecting road markings. Hautière et al. [7,9] estimate two kinds of visibility distances: meteorological visibility and mobilized visibility. The meteorological visibility is the greatest distance at which a black object of a suitable dimension can be seen in the sky on the horizon. The method [11] consists of dynamically implementing Koschmieder's law [16] and estimate the visibility based on local contrasts above 5%. The mobilized visibility represents the distance to the furthest pixel that still displays a contrast greater than 5%, which is very close to


J. Yang et al. (Eds.): CCCV 2017, Part I, CCIS 771, pp. 343–355, 2017.
https://doi.org/10.1007/978-981-10-7299-4_28

the meteorological visibility. They combine computations of a depth map and local contrasts above 5% to estimate the mobilized visibility [10]. This class of methods depends on an accurate geometric calibration of the camera. A second one correlates the contrast in the scene with the visual range estimated by reference additional sensors [8]. The geometric calibration is not necessary. The contrast can be simply calculated by a Sobel filter or a high-pass filter. Once the contrast is calculated, a linear regression is then performed to estimate the mapping function [14,21]. Such methods can be seen as data-driven approaches. Hautière et al. propose a probabilistic model-driven approach, which performs a simplified depth distribution model of the scene and applies a non-linear fitting to the data [3]. This class of methods needs a learning phase to estimate the mapping function, which requires collecting a large number of ground truth data. All of existing methods based on outdoor cameras rely on human assistance, like geometric calibration of the camera, road markings extraction or ground truth data collection for building mapping functions. Moreover, strict constraints for scene environments are essential for almost all methods, some of which even require the presence of just road and sky in the scene.

This paper proposes a novel method to estimate visibility just using a single image as input. According to the haze imaging model [12], a hi-quality haze-free image can be recovered, which makes it possible to obtain the ratio of two extinction coefficients respectively in current atmosphere and clear atmosphere by a single image. With the aim to calculate current atmosphere extinction coefficient, our work is inspired by the success of proposing an important prior-the clear atmosphere extinction coefficient is approximately a constant. It can be calculated by the theory of atmospheric radiation. By multiplying the clear atmosphere extinction coefficient and the ratio, the extinction coefficient of the input image is obtained and then the visibility is finally computed. Our method succeeds in estimating visibility in various application scenes by just a single image. The feasible results show high accuracy and robustness of this method, which might open a new trend of visibility measurement in meteorological research.

The remainder of this paper is organized as follows. Section 2 introduces our approach in details. Section 3 provides experimental results in various scenes and comparisons with existing approaches. A discussion and summary concludes this paper in Sect. 4.

## 2 Our Approach

The visibility calculation formula is proposed as follows [11]:

$$V_{met} = \frac{1}{\beta} ln \frac{1}{\varepsilon} \tag{1}$$

where $\varepsilon$ is contract threshold and equal to 5%. $\beta$ is extinction coefficient which indicates the scene radiance attenuated by the turbid atmosphere from a scene point to the sensor. The procedure of our method is depicted in Fig. 1. Based on

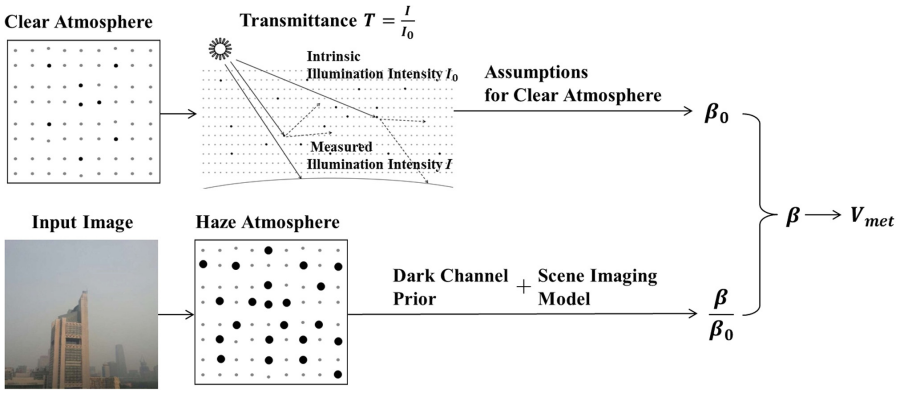


**Fig. 1.** Procedure of our method

a key observation of the clear atmosphere, we find that distributions of particles in clear atmosphere remain almost unchanged. Based on this, a conclusion is proposed that the clear atmosphere extinction coefficient $\beta_0$ is usually a constant. By introducing transmittance $T$, $\beta_0$ can be calculated combined with assumptions on clear atmosphere, which is developed by the theory of atmospheric radiation. Meanwhile, we advance the scene imaging model with dark channel prior to estimate $\beta/\beta_0$ of the input image. By multiplying $\beta_0$ and $\beta/\beta_0$ , the extinction coefficient $\beta$ is obtained and then the visibility is successfully calculated by Eq. (1). Moreover, the scene distance information of the input image also can be calculated as a by-product.

### 2.1 $\beta_0$ Calculation

The atmosphere is mainly composed of air molecules and aerosol particles. Air particles consist of nitrogen, oxygen, noble gas, carbon dioxide, water and other impurities. Aerosol is a suspension system of liquid or solid particles in the air. Only large-scale aerosol particles (e.g., dust, carbon, smoke particles) are sensitive to terrain, wind direction and other geographical factors [5], which affect visibility, climate and our health a lot. In the clear atmosphere, air molecules accounts for about 99% of the total atmosphere composition and the remaining 1% are small-scale aerosols. Experiments prove that the distribution of air particles remains unchanged within the height of 100 km [18]. Therefore, a reasonable assumption is proposed in this paper: the extinction coefficient in clear atmosphere is approximately a constant. We introduce transmittance $T$ to calculate $\beta_0$. Transmittance $T$ indicates the degree of solar radiation weakened in vertical direction [15]. The transmittance in clear atmosphere is defined by

$$T_0(\lambda, L) = e^{-\int_0^L \beta_0(\lambda, L) dl} \tag{2}$$

where $\lambda = 0.55\,\mu$m, L is the path length of solar radiation. The clear extinction coefficient $\beta_0$ consists of two parts: clear air molecular extinction coefficient $\beta_{R_0}$ and clear aerosol extinction coefficient $\beta_{\alpha_0}$

$$\beta_0 = \beta_{R_0} + \beta_{\alpha_0} \tag{3}$$

where $\beta_{R_0}$ is a known constant [18]: $1.159 \times 10^{-5}$(at $\lambda = 0.55\,\mu$m, and the unit is $m^{-1}$).With the aim to calculate $\beta_{\alpha_0}$ , the clear aerosol transmittance is described by

$$T_{\alpha_0}(\lambda, L) = e^{\int_0^L \beta_{\alpha_0}(\lambda, L)dl} \tag{4}$$

We introduce two assumptions on clear atmosphere to simplify the Eq. (4)

- Assume that the effective height of the atmosphere $H$ is $10^4$m. $10^4$m is the average height of troposphere including 80% of atmospheric particles and almost all the water vapor particles. In the height range higher than m, density coefficient of particle quantity is irrelevant to meteorological optical range [4].
- Assume the clear aerosol extinction coefficient is invariable. In the clear atmosphere, aerosol particle distributions are unaffected by airflow activities like convection and turbulence [1].

Based on above two assumptions, Eq. (4) is simplified as

$$T_{\alpha_0} = e^{-\beta_{\alpha_0} L} \tag{5}$$

By Eq. (5)

$$\beta_{\alpha_0} = -\frac{\log(T_{\alpha_0})}{L} \tag{6}$$

where $L = m_0 H$, $H = 10^4 m$. $m_0$ is relative optical mass [20], which is the ratio of path length of solar radiation and the effective height of the atmosphere(see Fig. 2). $m_0$ is calculated by

$$m_0 = \frac{1}{\cos\theta_s + 0.15 * (93.885 - \theta_s \frac{180}{\pi})^{-1.253}} \tag{7}$$

The solar zenith angle $\theta_\mathbf{s}$ indicates the position relationship of the sun and the earth, which is determined by the observation information: date, time and location [15].

$$t = t_s + 0.170\sin(\frac{4\pi(J-80)}{373}) - 0.129\sin(\frac{2\pi(J-8)}{355}) + \frac{12(SM-L)}{\pi} \tag{8}$$

$$\delta = 0.4093\sin(\frac{2\pi(J-81)}{368}) \tag{9}$$

$$\theta_s = \frac{\pi}{2} - \arcsin(\sin l \sin\delta - \cos l \cos\delta \cos\frac{\pi t}{12}) \tag{10}$$

where $t_s$ is observation time in decimal hours, $J$ is Julian date (the day of the year as an integer in the range 1–365), $L$ is site longitude in radians, $SM$ is standard meridian for the time zone in radians.

With the aim to calculate $\beta_{\alpha_\mathbf{0}}$, we introduce the clear aerosol transmittance formula proposed by Ångström [2]

$$T_{\alpha_0} = e^{-\beta_A m_0 \lambda^{-\alpha_w}} \tag{11}$$

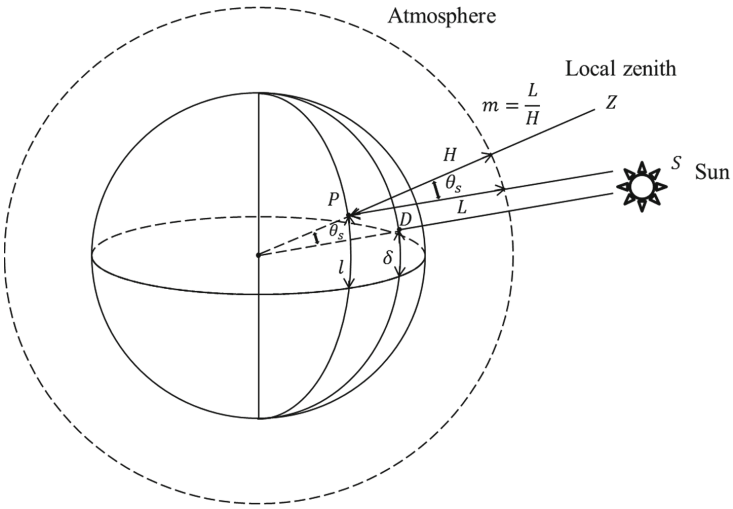


**Fig. 2.** Diagram of relative optical mass. $P$ is the site point, $D$ is the under-solar point, $l$ is site latitude in radians, $\delta$ is solar declination, $\theta_s$ is solar zenith angle.

where $\beta_A$ is Ångströms turbidity coefficient indicating the level of atmospheric turbidity. The value range of $\beta_A$ is $0.01 \leq \beta_A \leq 0.2$ [2]. $\alpha_w$ is wavelength exponent reflecting the distribution characteristics of aerosol particle spectrum. The value range of $\alpha_w$ is $0.1 \leq \beta_A \leq 4$ [6]. When the proportion of small particles increases, the value of also grows. In pure atmosphere, air molecules accounts for about 99% of atmosphere constituents, which has almost reached a limit condition of atmosphere. So we take the minimum value of $\beta_A$ and the maximum value of $\alpha_w$ to Eq. (11). Combining with Eq. (11), Eq. (6) becomes

$$\beta_{\alpha_0} = \frac{\beta_A m_0 \lambda^{-\alpha_w}}{L} \tag{12}$$

where $L = m_0 H$

$$\beta_{\alpha_0} = \frac{\beta_A \lambda^{-\alpha_w}}{H} \tag{13}$$

where $m_0$ is significantly omitted, which proves that $\beta_{\alpha_0}$ is independent on observation information (date, time and location) and always a constant. Based on Eq. (3), we finally calculate $\beta_0 : 2.2518 \times 10^{-5} m^{-1}$.

### 2.2 $\beta/\beta_0$ Calculation

In this paper, we combine the dark channel prior [12] and the improved scene imaging model to deduce $\beta/\beta_0$. The dark channel prior is a kind of statistics of haze-free outdoor images–in clear atmosphere, most local patches contain some pixels which have very low intensities in at least one color channel. For an image $I$, the dark channel is defined by

$$I_{\Omega(x)}^{dark} = \min_{c\in\{r,g,b\}} \left( \min_{y\in\Omega(x)} I^c(y) \right) \tag{14}$$

where c is a color channel. $\Omega(x)$ is a local patch centered at x. The patch size is 15×15 in this paper. Based on the statistics of 1000 outdoor images, we find that $I^{dark}$ increase with the aggravation of the atmosphere turbidity. The patch with the minimum $I^{dark}$ at other levels of atmosphere turbidity corresponds to the minimum one in clear atmosphere, which satisfies the dark channel prior most. Therefore, we take the min operation on Eq. (10) to select the minimal dark channel patch $\Omega_{min}(x)$ in the input image $I$ (see Fig. 3[1st column]):

$$\hat{I_{\Omega_{\min}(x)}^{dark}} = \min_{x\in I}( \min_{c\in\{r,g,b\}} ( \min_{y\in\ \Omega(x)} (I^{dark}(y)))) \tag{15}$$

We refine $\Omega_{min}(x)$ using guided filter [13](see Fig. 3[2nd column])

$$I_{\Omega_{\min}(x)}^{dark} = guidedfilter(\hat{I_{\Omega_{\min}(x)}^{dark}}) \tag{16}$$

Figure 3 [2nd column] shows that patches in $\Omega_{\min}(x)$ may be not at the same distance, and $I_{\Omega_{\min}(x)}^{dark}$ are probably unequal in a patch due to the block effects, which will influence the following calculation for $\beta/\beta_0$. Therefore, we need to improve $\Omega_{\min}(x)$. The specific process is as follows:

- Select the minimal value $V_{\min}$ of $I_{\Omega_{\min}(x)}^{dark}$.
- Retrieve all connected regions of $\Omega_{\min}(x)$ and find the $\Omega_{\min}(x_{\min})$ containing $V_{\min}$. Note that the number of regions in $\Omega_{\min}(x_{\min})$ is always more than one.
- Traverse the $\Omega_{\min}(x_{\min})$ and calculate $\left| I_{\Omega_{\min}(x_{\min})}^{dark}(y) - V_{\min} \right|$ where $y = 1, 2 \cdots n$, $n \in \Omega_{\min}(x_{\min})$. If $\left| I_{\Omega_{\min}(x_{\min})}^{dark}(y) - V_{\min} \right| \geq T$, y is supposed as a false pixel and omitted. We fix the T to 0.2 in this paper.
- Count the number of each remaining regions in $\Omega_{\min}(x_{\min})$ and eliminate the noise region whose quantity of pixels is less than $N_{num}$. We fix the $N_{num}$ to 5% of the total number of $\Omega_{\min}(x)$ in this paper.

The resulting regions are almost at the same distance and satisfy the dark channel prior most, which are supposed to be the *ROI* ((see Fig. 3[3rd column])). Next we will calculate $\beta/\beta_{\mathbf{0}}$ of this *ROI*.

For an outdoor image, a model [17] is widely used to describe the imaging process (see Eq. (13)). Note that the atmosphere is homogenous

$$I = \rho I_\infty e^{-\beta d} + I_\infty (1 - e^{-\beta d}) \tag{17}$$

where $I$ is scene image, $\rho$ is scene albedo. $I_\infty$ is air light, which is invariant with $\beta$ and determined only by the illumination intensity. $\rho I_\infty$ is scene radiance, $I_\infty$ is medium transmission. Based on Eq. (13), the scene imaging in clear atmosphere is easily derived by

$$J = \rho I_\infty e^{-\beta_0 d} + I_\infty (1 - e^{-\beta_0 d}) \tag{18}$$

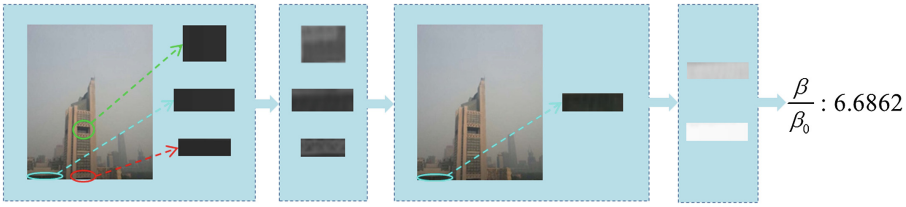


**Fig. 3.** Procedure of $\beta/\beta_0$ Calculation. [1st column] result of $\Omega_{\min}(x)$ and $I^{\hat{dark}}_{\Omega_{\min}(x)}$. [2nd column] result of $I^{dark}_{\Omega_{\min}(x)}$. [3rd column] result of $ROI$. [4th column] the above result is $e^{-(\beta-\beta_0)d}(y)$ and the below result is $e^{-\beta_0 d}(y), y \in ROI$. [5th column] result of $\beta/\beta_0$.

where $J$ is intrinsic scene image. Combine Eq. (13) with Eq. (14), the advanced scene imaging model is obtained:

$$J = Je^{-(\beta-\beta_0)d} + I_\infty(1 - e^{-(\beta-\beta_0)d}) \tag{19}$$

By Eq. (15), we find that when $\beta$ decreases to $\beta_0$ , scene image $I$ is recovered to $J$. Compared with previous model-driven methods for haze removal, this restoring process retains the fundamental cue for human to perceive depth. So we use Eq. (15) to recover $J$ and calculate $\beta/\beta_0$. According to the dark channel prior, the dark channel of scene radiance tends to be 0.

$$\min_{c\in\{r,g,b\}}\left(\min_{y\in ROI}\left(\rho I^c_\infty(y)\right)\right) = 0 \tag{20}$$

Note that the clear atmosphere is composed of air molecules and a few small-scale aerosol particles. So the dark channel of the intrinsic scene intensity is close to 0.

$$\min_{c\in\{r,g,b\}}\left(\min_{y\in ROI}\left(J^c_\infty(y)\right)\right) = \mu \tag{21}$$

where $\mu$ should be very close to 0, so we fix it to 0.001 in this paper. $e^{-\beta_0 d}$ and $e^{-(\beta-\beta_0 d)}$ are obtained by

$$e^{-\beta_0 d}(y) = guidedfilter(1 - \min_{c\in\{r,g,b\}}(\min_{y\in\ ROI}(\frac{J^c(y)}{I^c_\infty}))) \tag{22}$$

$$e^{(\beta-\beta_0)d}(y) = guidedfilter((1 - \min_{c\in\{r,g,b\}}(\min_{y\in\ ROI}(\frac{I^c(y)}{I^c_\infty})))/(1 - \frac{\mu}{I^c_\infty})) \tag{23}$$

where $I_\infty$ can be estimated by [12] and $J$ is recovered by:

$$J(y) = \frac{I(y) - I_\infty}{\max(e^{-(\beta-\beta_0)d}(y), t_0)} + I_\infty, y \in ROI \tag{24}$$

where $t_0$ is a lower bound 0.1 in case $e^{-(\beta-\beta_0)d}$ decrease down to 0. Figure 3[4th column] shows the results of $e^{(\beta-\beta_0)d}$ and $e^{-\beta_0 d}$. Then $\beta/\beta_0(y)$ is computed by

$$\frac{\beta}{\beta_0}(y) = \frac{\ln(e^{-(\beta-\beta_0)d})}{\ln(e^{-\beta_0 d})}(y) + 1 \tag{25}$$

We take the average value of $\beta/\beta_0(y)$ in $ROI$ (see Fig. 3[5th column]). Based on Eq. (1), visibility $V_{met}$ is finally obtained by

$$V_{met} = \frac{1}{\beta_0 \times \frac{\beta}{\beta_0}} \ln \frac{1}{\varepsilon} \tag{26}$$

## 3 Experimental Results

In our experiment, there are three kinds of scenes: city scene, road scene and nature scene. We use the visibility $V_{met}^{ob}$ provided by Yahoo!Weather as a criterion of the experimental results. We define the error rate $E$ by

$$E = \frac{\left|V_{met} - V_{met}^{ob}\right|}{V_{met}^{ob}} \tag{27}$$

If error rate is less than 20%, the result is acceptable.

Figure 4 shows the experimental images in city scenes at different levels of atmosphere turbidity. As can be seen, the variance of atmosphere turbidity in city scene is mainly caused by air pollution. Visibility is a good indicator of city's air quality. Figures 5 and 6 show the experimental images in road scenes and nature scenes at different levels of atmosphere turbidity. Tables 1, 2 and 3 shows the visibility results of Figs. 4, 5 and 6. Error rates in different kinds of scenes are less than 20%, which demonstrates the high accuracy of our method. Moreover, our method preforms well without human assistance. [More results can be found at http://airl.csu.edu.cn/airquality.html]

**Table 1.** Visibility results of Fig. 4

| Instance | F4-1 | F4-2 | F4-3 | F4-4 |
|---|---|---|---|---|
| $V_{met}$[m] | 19645.0 | 8782.0 | 2895.5 | 985.0 |
| $V_{met}^{ob}$[m] | 24000 | 8000 | 3000 | 1000.0 |
| $E$[%] | 18.1 | 9.8 | 3.5 | 1.5 |

**Table 2.** Visibility results of Fig. 5

| Instance | F5-1 | F5-2 | F5-3 | F5-4 |
|---|---|---|---|---|
| $V_{met}$[m] | 20972.6 | 7436.2 | 319.6 | 31.5 |
| $V_{met}^{ob}$[m] | 24000.0 | 8000.0 | 300.0 | 30.0 |
| $E$[%] | 12.6 | 7.1 | 6.5 | 5.0 |

**Table 3.** Visibility results of Fig. 6

| Instance | F6-1 | F6-2 | F6-3 | F6-4 |
|---|---|---|---|---|
| $V_{met}$[m] | 19267.7 | 16205.3 | 9529.5 | 5840.8 |
| $V_{met}^{ob}$[m] | 24000.0 | 15000.0 | 9000.0 | 6000.0 |
| $E$[%] | 19.72 | 8.04 | 5.88 | 2.65 |

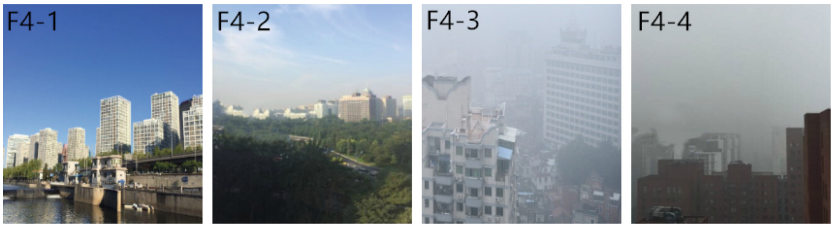


**Fig. 4.** Experimental images in different city scenes

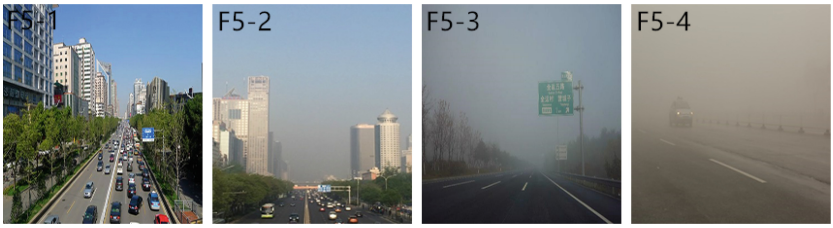


**Fig. 5.** Experimental images in the road scene

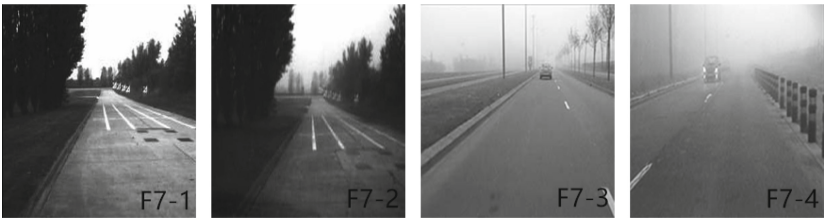


**Fig. 6.** Experimental images in nature scenes

This paper also adopts Hautière N's two popular methods [9,11] as comparison objects (see Fig. 7). Method [9] based on in-vehicle cameras describes two specific onboard techniques to estimate the meteorological visibility and the mobilized visibility. We only consider the meteorological visibility in this paper. Method [11] consists of dynamically implementing Koschmieder's law and estimate the visibility based on local contrasts above 5%. $V_{met}^{H}$represents the visibility estimated by Hautière N's methods. In Table 4, error rates of our

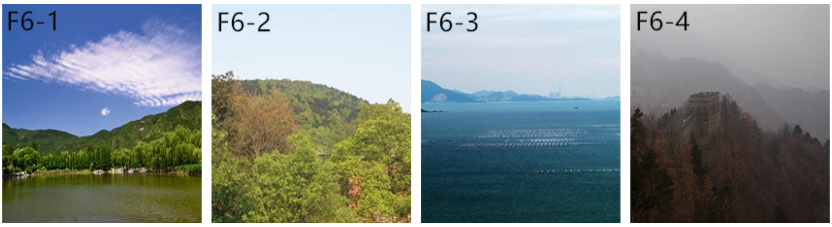


**Fig. 7.** Comparisons with Hautière N's work [9,11]

method are all less than 20%. Our results are comparable with Hautière N's in the road scene. Furthermore, our method is also applicable to other types of scenes, which is better than Hautière N's methods. Our approach even works for distance estimation. Having obtained $\beta$ , we can calculate the distance from the scene point to the sensor according to Eq. (28)

$$d = \frac{\log(e^{-(\beta-\beta_0)d})}{\beta_0 - \beta} \tag{28}$$

**Table 4.** Experimental results compared with Hautière N's methods

| Instance | $V_{met}$[m] | $V_{met}^{ob}$[m] | $V_{met}^{H}$[m] | $E$[%] |
|---|---|---|---|---|
| F7-1 | 4078.8 | 5000.0 | 4753.7 | 18.42 |
| F7-2 | 2291.0 | 2000.0 | 1903.7 | 14.55 |
| F7-3 | 351.9 | 400.0 | 436.0 | 12.03 |
| F7-4 | 42.5 | 40.0 | 43.0 | 6.25 |

In order to prove the above algorithm, we collect a specific scene(see Fig. 8). The building marked by a red circle is the China Central Television in Beijing, which is about 200 m far from the camera. The building marked by a green circle

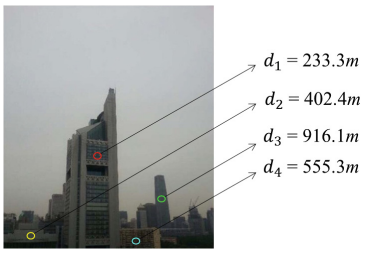


**Fig. 8.** Distance results in the same scene at different scene points

is the China World Trade Center Tower 3, which is about 1000 m far from the sensor. Figure 8 shows the distance results at four different scene points. Note that distances for reference at the four scene points are as follows: $d_1 \approx 200$ m, $d_2 \approx 400$ m, $d_3 \approx 1000$ m and $d_4 \approx 500$ m. Results show that calculated distances are close to the reference data, which proves the rationality of this method. Unlike other camera calibration methods, our method merely depends on an outdoor image, which is simple and cost-effective. This method might have an important propelling effect on field measurement in outdoor scenes.

## 4 Conclusion

In this paper, we propose a novel method for visibility estimation using a single image. A key assumption is developed - the extinction coefficient is approximately a constant in clear atmosphere which is composed of air molecules and a few small-scale aerosol particles. Using this assumption with the dark channel prior, the extinction coefficient of the input image can be calculated and the visibility is finally obtained. Without human assistance, the feasible results prove high accuracy and robustness, which might open a new trend in meteorological research on visibility measurement.

Compared with existing visibility measurements, our method has the following advantages:

- This method proposes an assumption for calculating the clear extinction coefficient and realizes the separation of extinction coefficient $\beta$ and distance d in depth map $\beta d$, which makes it true that the visibility estimation no longer relies on the actual distance information.
- This method depends on a single image and successfully accomplishes fully automatic visibility estimation without human assistance, which performs well in various types of scene.
- This method makes it possible to measure scene distance using a single image, which might open a new trend in meteorological research about scene distance measurement.

Our method proposes a framework to estimate the visibility, which is based on an algorithm of single image haze removal. With the development of haze removal technology, other new methods may be proposed. Therefore, our future work is to explore the possibility of other methods to calculate $\beta/\beta_0$.

**Acknowledgments.** This research was supported by the National Natural Science Foundation of China(No. 61602520), the Fundamental Research Funds for the Central Universities of Central South University(No. 2017zzts500)

## References


1. Anderson, G.P., Berk, A., Acharya, P.K., et al.: MODTRAN4: radiative transfer modeling for remote sensing. Proceedings of SPIE - The International Society for Optical Engineering **3866**(1), 1029–1032 (1999)
2. Ångström, A.: The parameters of atmospheric turbidity. Tellus **16**(1), 64–75 (1964)
3. Babari, R., Hautière, N., Dumont, E., Papelard, J.P.: Computer vision for the remote sensing of atmospheric visibility. In: 2011 IEEE International Conference on Computer Vision Workshops (ICCV Workshops), pp. 219–226. IEEE (2011)
4. Berk, A., Anderson, G.P., et al.: MODTRAN 5: a reformulated atmospheric band model with auxiliary species and practical multiple scattering options: update. In: Defense and Security, pp. 662–667. International Society for Optics and Photonics (2005)
5. Bohren, C.F., Huffman, D.R.: Absorption and Scattering of Light by Small Particles. Wiley, Hoboken (2008)
6. Calinoiu, D.G., Stefu, N., Paulescu, M., et al.: Evaluation of errors made in solar irradiance estimation due to averaging the Angstrom turbidity coefficient. Atmos. Res. **150**(1), 69–78 (2014)
7. Gallen, R., Hautière, N., Cord, A., et al.: Supporting drivers in keeping safe speed in adverse weather conditions by mitigating the risk level. IEEE Trans. Intell. Transp. Syst. **14**(4), 1558–1571 (2013)
8. Hallowell, R., Matthews, M., Pisano, P.: An automated visibility detection algorithm utilizing camera imagery. In: 23rd Conference on Interactive Information and Processing Systems for Meteorology, Oceanography, and Hydrology (IIPS) (2007)
9. Hautière, N., Aubert, D., Dumont, E., et al.: Experimental validation of dedicated methods to in-vehicle estimation of atmospheric visibility distance. IEEE Trans. Instrum. Meas. **57**(10), 2218–2225 (2008)
10. Hautière, N., Labayrade, R., Aubert, D.: Estimation of the visibility distance by stereovision: a generic approach. IEICE Trans. Inf. Syst. **89**(7), 2084–2091 (2006)
11. Hautière, N., Tarel, J.P., Lavenant, J., Aubert, D.: Automatic fog detection and estimation of visibility distance through use of an onboard camera. Mach. Vis. App. **17**(1), 8–20 (2006)
12. He, K., Sun, J., Tang, X.: Single image haze removal using dark channel prior. IEEE Trans. Pattern Anal. Mach. Intell. **33**(12), 2341–2353 (2011)
13. He, K., Sun, J., Tang, X.: Guided image filtering. IEEE Trans. Pattern Anal. Mach. Intell. **35**(6), 1397–1409 (2013)
14. Liaw, J.-J., Lian, S.-B., Huang, Y.-F., Chen, R.-C.: Atmospheric visibility monitoring using digital image analysis techniques. In: Jiang, X., Petkov, N. (eds.) CAIP 2009. LNCS, vol. 5702, pp. 1204–1211. Springer, Heidelberg (2009). https://doi.org/10.1007/978-3-642-03767-2_146
15. Liou, K.N.: An Introduction to Atmospheric Radiation, vol. 84. Academic press, Cambridge (2002)
16. Middleton, W.E.K.: Vision through the atmosphere. In: Bartels, J. (ed.) Geophysik II / Geophysics II. HPEP, vol. 10/48, pp. 254–287. Springer, Heidelberg (1957). https://doi.org/10.1007/978-3-642-45881-1_3
17. Narasimhan, S.G., Nayar, S.K.: Vision and the atmosphere. Int. J. Comput. Vis. **48**(3), 233–254 (2002)
18. Patterson, M.S., Chance, B., Wilson, B.C.: Time resolved reflectance and transmittance for the noninvasive measurement of tissue optical properties. Appl. opt. **28**(12), 2331–2336 (1989)

19. Pomerleau, D.: Visibility estimation from a moving vehicle using the Ralph vision system. In: IEEE Conference on Intelligent Transportation System, ITSC 1997, pp. 906–911. IEEE (1997)
20. Preetham, A.J., Shirley, P., Smits B.: A practical analytic model for daylight. In: Proceedings of the 26th Annual Conference on Computer Graphics and Interactive Techniques, pp. 91–100. ACM Press/Addison-Wesley Publishing Co. (1999)
21. Xie, L., Chiu, A., Newsam, S.: Estimating atmospheric visibility using general-purpose cameras. In: Bebis, G., et al. (eds.) ISVC 2008. LNCS, vol. 5359, pp. 356–367. Springer, Heidelberg (2008). https://doi.org/10.1007/978-3-540-89646-3_35